

## Integrin-Free Tetraspanin CD151 Can Inhibit Tumor Cell Motility upon Clustering and Is a Clinical Indicator of Prostate Cancer Progression

Trenis D. Palmer<sup>1</sup>, Carlos H. Martínez<sup>4</sup>, Catalina Vasquez<sup>3</sup>, Katie E. Hebron<sup>1,2</sup>, Celestial Jones-Paris<sup>1</sup>, Shanna A. Arnold<sup>1</sup>, Susanne M. Chan<sup>4</sup>, Venu Chalasani<sup>4</sup>, Jose A. Gomez-Lemus<sup>5</sup>, Andrew K. Williams<sup>3</sup>, Joseph L. Chin<sup>4</sup>, Giovanna A. Giannico<sup>1</sup>, Tatiana Ketova<sup>1</sup>, John D. Lewis<sup>3</sup>, and Andries Zijlstra<sup>1,2</sup>

### Abstract

Normal physiology relies on the organization of transmembrane proteins by molecular scaffolds, such as tetraspanins. Oncogenesis frequently involves changes in their organization or expression. The tetraspanin CD151 is thought to contribute to cancer progression through direct interaction with the laminin-binding integrins  $\alpha 3\beta 1$  and  $\alpha 6\beta 1$ . However, this interaction cannot explain the ability of CD151 to control migration in the absence of these integrins or on non-laminin substrates. We demonstrate that CD151 can regulate tumor cell migration without direct integrin binding and that integrin-free CD151 (CD151<sup>free</sup>) correlates clinically with tumor progression and metastasis. Clustering CD151<sup>free</sup> through its integrin-binding domain promotes accumulation in areas of cell–cell contact, leading to enhanced adhesion and inhibition of tumor cell motility *in vitro* and *in vivo*. CD151<sup>free</sup> clustering is a strong regulator of motility even in the absence of  $\alpha 3$  expression but requires PKC $\alpha$ , suggesting that CD151 can control migration independent of its integrin associations. The histologic detection of CD151<sup>free</sup> in prostate cancer correlates with poor patient outcome. When CD151<sup>free</sup> is present, patients are more likely to recur after radical prostatectomy and progression to metastatic disease is accelerated. Multivariable analysis identifies CD151<sup>free</sup> as an independent predictor of survival. Moreover, the detection of CD151<sup>free</sup> can stratify survival among patients with elevated prostate-specific antigen levels. Cumulatively, these studies demonstrate that a subpopulation of CD151 exists on the surface of tumor cells that can regulate migration independent of its integrin partner. The clinical correlation of CD151<sup>free</sup> with prostate cancer progression suggests that it may contribute to the disease and predict cancer progression. *Cancer Res*; 74(1); 173–87. ©2013 AACR.

### Introduction

Cancer metastasis typically involves the migration and invasion of disseminating tumor cells. The activity of cytokine receptors, adhesion receptors, and proteases responsible for this migration, is frequently controlled through their organization within the cell membrane. Tetraspanins are key membrane scaffolding proteins responsible for this organization. Although the tetraspanins lack enzymatic activity and canonical signal-transducing capacity, their ability to organize mac-

romolecular structures is their primary mechanism of action (1). Of the 33 tetraspanin family members, 6 have been implicated in cancer (2, 3) and CD151 has been shown to be a particularly important regulator of tumor cell motility (4) and metastasis (5, 6). CD151 interacts with several partners, including matrix metalloproteinase (MMP-14), cadherins, immunoglobulin proteins, and integrin subunits  $\alpha 3$  and  $\alpha 6$ , as well as other members of the tetraspanin family (1, 7, 8). Consequently, further elucidation of tetraspanin function requires investigation of its molecular organization and the role of specific partners. The interaction between CD151 and the laminin-binding integrins  $\alpha 3\beta 1$  and  $\alpha 6\beta 1$  has been investigated in detail (reviewed in refs. 1 and 9). Loss of CD151 (10) diminished migration on laminin, whereas disruption of the integrin-binding domain limits spreading on laminin and tubule morphogenesis as well as tumor growth in three-dimensional laminin-containing matrixes (11, 12). Recently, the CD151-integrin-laminin axis has been shown to facilitate EGF signaling (13, 14). However, a number of biologic activities have been associated with CD151 that are likely to involve different molecular mechanisms. These include migration on non-laminin substrates, platelet function, and cell–cell adhesion. Effective approaches to investigating these functions have included genomic ablation (14–16), mutational analysis (11, 17, 18), and

**Authors' Affiliations:** Departments of <sup>1</sup>Pathology, Microbiology and Immunology and <sup>2</sup>Cancer Biology, Vanderbilt University, Nashville, Tennessee; <sup>3</sup>Department of Oncology, University of Alberta, Edmonton, Alberta; <sup>4</sup>Translational Prostate Cancer Research Group, London Regional Cancer Program; and <sup>5</sup>Department of Pathology, Schulich School of Medicine and Dentistry, The University of Western Ontario, London, Ontario Canada

**Note:** Supplementary data for this article are available at Cancer Research Online (<http://cancerres.aacrjournals.org/>).

**Corresponding Authors:** John D. Lewis, University of Alberta, 5-142C Katz Group Building, 114th St and 87th Ave., Edmonton, AB T6G 2E1 Canada; E-mail: jdl@ualberta.ca; Andries Zijlstra, Vanderbilt University Medical Center, 1161 21st Ave. S., C-2102c MCN, Nashville, TN 37232-2561. Phone: 615-322-3295; Fax: 615-936-7040; E-mail: Andries.Zijlstra@vanderbilt.edu

doi: 10.1158/0008-5472.CAN-13-0275

©2013 American Association for Cancer Research.

CD151-specific antibodies (6, 19, 20). These studies suggest that both integrin-dependent and integrin-independent roles exist for CD151 in tumor progression.

CD151 can be targeted to inhibit tumor cell motility and metastasis using the antibody mAB 1A5 (6). Treatment with mAB 1A5 prevents deadhesion at the rear of migrating cells, resulting in their immobilization and subsequent inhibition of metastatic dissemination (6). mAB 1A5, like most anti-CD151 antibodies, was generated in mice against a human antigen (20). Consequently, these antibodies primarily recognize antigenic differences between human and mouse CD151. Some CD151 antibodies exhibit differential staining patterns in human tissues most likely because certain epitopes are masked by protein-protein interactions of the CD151 complex (11, 21–24). Epitope mapping allows these antibodies to identify the composition of a CD151 complex. Yamada and colleagues (19) used flow cytometry to map epitope binding of CD151 antibodies on CD151 mutants with substitutions at amino acid residues that are not conserved between human and mouse CD151. These studies demonstrated that several antibodies recognize an epitope on CD151 required for binding integrins, including  $\alpha 3 \beta 1$  (11). Interestingly, the knockdown of  $\alpha 3$  reduced to the overall level of CD151 but did not diminish the level of CD151 recognized by antibodies to the integrin-binding domain. This observation suggests that distinct populations of CD151 are maintained on the cell surface. One of those populations is associated with integrins while the other is not. We will refer to these populations as CD151<sup>ITGA</sup> and CD151<sup>free</sup>, respectively.

Considering the epitope-specificity of antibodies, it is likely that antibodies that recognize distinct CD151-partner complexes can provide insight into the function and clinical relevance of that CD151 subpopulation. We hypothesized that the inhibition of motility in response to mAB 1A5 was due to its ability to target a specific subpopulation of CD151 and affects its activity. Since a monovalent fragment of mAB 1A5 was unable to inhibit tumor cell motility, we predicted that this antibody-mediated clustering of all, or a specific subpopulation of CD151. Live-cell imaging was implemented to investigate clustering in response to antibody binding. Using the flow cytometry approach developed by Yamada and colleagues, we determined that mAB 1A5 recognized the integrin-binding domain on CD151 and is therefore unable to interact with integrin-bound CD151. The analysis of tumor cell migration *in vivo* was used to investigate the ability of mAB 1A5 to control cell motility independent of integrin  $\alpha 3$ . These investigations were extended to other antibodies that recognize the same integrin-binding domain (8C3 and 14A2.H1) or bind an unrelated site (11G5A). Finally, we determined whether the presence CD151 not bound by integrins was relevant in prostate cancer progression by histologic analysis of CD151<sup>free</sup> in tissue from two cohorts of patients with prostate cancer.

## Materials and Methods

### Cell culture, reagents, and antibodies

HEp3 cells are perpetually maintained on the chick chorioallantoic membrane to retain metastatic and migratory poten-

tial (25, 26). All cell lines were grown in media supplemented with penicillin/streptomycin, sodium pyruvate, nonessential amino acids, and 10% FBS and cultured at 37°C in 5% CO<sub>2</sub> incubator and passaged every 2 to 4 days. HEp3, NIH3T3, and HT1080 cells were maintained in Dulbecco's Modified Eagle Medium (DMEM). A549 cells were maintained in RPMI. The CD151 plasmids in the eGFP-N1 vector (Clontech) were received from Dr. Kiyo Sekiguchi (University of Osaka, Japan). Transfections of all cells were performed using Extreme Gene HD (Roche). The mAB 1A5 and the control antibody 29-7 was generated as described previously (27). The anti-CD151 antibodies 11G5A and 14H2.1 were purchased from Abcam. Anti-CD151 antibody 8C3 was generously provided by Dr. Sekiguchi. Anti- $\alpha 3$  antibodies were purchased from Santa Cruz Biotechnology (PIB5) and Millipore. The smart pool RNAi specific to  $\alpha 3$ , PKC $\alpha$ , and the control siRNA was obtained from Dharmacon.

### Tumor cell motility

***In vitro cell migration.*** HEp3 and HT1080 cells were seeded in 6-well plates and allowed to attach overnight in DMEM containing 10% FBS. On the following day, the cells were switched to serum-free/insulin-free media for an additional 24 hours. On the day of the assay, the confluent monolayers were scratched with a pipette tip to create a uniform wound, after which the cells were washed with PBS to remove any floating cells. Cultures were returned to full medium and the wound was documented at 0 hours and 16 hours post-scratch using a light microscope TMS-F (Nikon) equipped with a D90 SLR camera (Nikon). Wound closure (% surface area) was determined using T-scratch image analysis software (28).

***In vivo cell motility.*** Assays were performed as previously described (6). Briefly, cells to be injected were washed 2 times with PBS and detached with 2 mmol/L EDTA. The cells were resuspended in PBS and injected intravenously into day 12 chick embryos. Four days after injection, the disseminated colonies were photographed using a Lumar V12 stereomicroscope (Zeiss) equipped with a Retiga Exi camera and controlled with Volocity image acquisition software (PerkinElmer). Antibody treatments were introduced by intravenous injection one day after tumor cell injection. For visualization of the vasculature, rhodamine-conjugated dextran was injected intravenously and allowed to circulate for 15 minutes before tissue collection. "Non-motile" colonies were defined as colonies composed of 5 or more cells where individual cells remained in direct contact. Such non-motile colonies are compact, whereas "motile" colonies contained a migratory cell populations dispersed in the CAM. Assays were performed with 5 animals per treatment and 5 or more fields per animal analyzed for colony formation. Data are represented as the percentage of colonies within a single animal that demonstrated a motile phenotype.

### Flow cytometry

***Standard flow procedure.*** Cells to be used in flow cytometry experiments were trypsinized with 0.25% Trypsin-EDTA and resuspended in cold Milytenyi FACS buffer (2 mmol/L EDTA, 0.5% BSA, PBS). For the analysis of cell surface

expression of specific antigens, the cells were washed 2 times with fluorescence-activated cell sorting (FACS) buffer and then stained with the specific primary antibodies for 1 hour on ice. Following incubation with the primary antibody, the cells were washed 2 times with cold FACS buffer and then incubated with species-specific, fluorophore-conjugated secondary antibody.

**Epitope mapping using flow cytometry.** NIH 3T3 were transfected with the CD151 human/mouse GFP substitution mutants (19) using Fugene HD (Roche). Transfected cells were prepared for flow cytometry as described above 24 hour after transfection. Cells were stained with anti-CD151 antibodies (mAB 1A5, 8C3, 14A2H.1, and 11G5A) on ice for 1 hour followed by two washes and incubation with Alexa 647-conjugated secondary antibody (1 hour on ice). The stained cells were washed twice with cold FACS buffer, resuspended, and analyzed by two-color flow cytometry. Untransfected controls and empty vector (pEGFP N1) transfections were used as a no color and GFP-only-positive controls, respectively. An isotype IgG was used for as a control for gating purposes. To analyze the GFP-positive and Alexa 647 double-positive populations, the cells were gated for GFP expression to identify GFP-expressing cells that were subsequently analyzed for their binding of Alexa 647-conjugated antibody (which represents binding of the respective anti-CD151 antibody). The data are presented as dot plots with the detection of GFP graphed on the *x*-axis and the detection of Alexa 647 plotted on the *y*-axis.

#### Immunoprecipitation, immunoblotting, and immunodepletion

**Immunoprecipitation.** HEp3 cells and A549 cells were lysed in either 1% (v/v) Triton X-100 lysis buffer or 1% (v/v) Brij-99 lysis buffer on ice for 30 minutes. The samples were cleared by centrifugation (14,000 rpm, 15 minutes) and cleared lysates were transferred to new tubes and stored at 4°C. Protein concentrations were determined by BCA (Pierce). Immunoprecipitations were performed by incubating 2 µg of the antibody with 1 mg total cell lysate overnight at 4°C with end-to-end rotation. The following day, the protein/antibody complexes were bound to Protein A/G Sepharose Beads (Fisher Scientific) for 4 hours at 4°C with end-to-end rotation. Beads were collected by centrifugation (8,000 rpm, 30 seconds), washed with lysis buffer, and stored together with unbound material for further analysis. Immunoprecipitated complexes were eluted in 100 µL Lamelli sample buffer and evaluated by immunoblotting. For each sample, equal amounts of protein were loaded into SDS-PAGE and blotted onto polyvinylidene difluoride membranes (PVDF, Millipore). Protein detection was performed with enhanced chemiluminescence (ECL, Pierce) after blocking (5% non-fat milk from powder in PBS, 0.05% Tween-20) and incubation (O/N 4°C) with antibodies prepared in blocking buffer.

**Immunodepletion of mAB 1A5-bound CD151.** (i) HEp3 or A549 cells were lysed in 1% Triton X-100 lysis buffer and incubated with 2 µg of antibody for 2 hours at 4°C with end-to-end rotation. The immunocomplexes were then captured with Protein-G sepharose beads for 1 hour at 4°C. This process was repeated 3 times using the unbound lysate. Each

immunodepletion was evaluated by immunoblotting as described above. (ii) For immunodepletion of mAB 1A5 bound to live cells, HEp3 and A549 cells were treated overnight with mAB 1A5 or control antibody at a concentration of 2 µg/mL. Antibody-bound cells were lysed 24 hours later and antibody-bound CD151 was immunodepleted with protein-G sepharose beads. The unbound material was depleted 2 additional times with protein-G beads and bound as well as unbound material was evaluated by immunoblotting.

**Cell surface biotinylation.** For cell surface labeling, confluent HEp3 cells were treated with antibody for 1 hour on ice and then washed 3 times with cold PBS. Cultures were subsequently biotinylated with sulfo-succinimidyl-6-[biotin-amido]hexanoate using the EZ-Link Sulfo-NHS-Biotinylation Kit (Thermo Scientific) according to the manufacturer's instructions. Cells were lysed in either 1% Brij 99 followed by extraction of the insoluble material with radioimmunoprecipitation assay (RIPA) buffer. Immunoprecipitation was performed as described above. Biotinylated proteins were detected with peroxidase-conjugated streptavidin.

#### Live-cell imaging and immunofluorescent staining

To visualize CD151 localization, HEp3 cells expressing GFP-tagged CD151 were imaged with a fully automated microscope (BX61, Olympus) equipped with a digital camera (Orca ER, Hamamatsu) every 5 minutes for 1 hour. Cells were subsequently treated with Alexa 647-conjugated mAB 1A5 and imaging continued for an additional 3 hours. Movies were analyzed and compiled using Volocity Image Acquisition and Analysis Software (PerkinElmer).

Immunofluorescent detection of anti-CD151 antibodies bound to cultured cells was accomplished by staining paraformaldehyde fixed cells with Alexa 546-conjugated secondary antibody. Fibronectin fibrillogenesis was detected on paraformaldehyde-fixed cells by immunofluorescent staining with rabbit anti-fibronectin antibody in conjunction with Alexa 546-conjugated anti-rabbit secondary antibodies. Images were captured with a fluorescent microscope using Volocity Image Acquisition and Analysis Software (PerkinElmer).

#### Platelet aggregation assay

Platelet aggregation assays were performed as previously described (29). Blood to be used from donors was collected and mixed 1:10 with 3.8% sodium citrate buffer and spun at 160 × *g* for 30 minutes. The platelet-rich plasma (PRP) was counted and resuspended at a concentration of 2–4 × 10<sup>8</sup> cells/mL. Aggregation of PRP was performed on a BIO/DATA Corporation PAP-4 aggregometer at 37°C with stirring (1,200 rpm). Individual treatments were added as outlined in the text and turbidity analyzed compared with the aggregation of platelet poor plasma.

#### Cell clustering assay

Suspension cultures of Jurkat and U937 cells were treated with control antibody or mAB 1A5 overnight using serum-free culture medium. Clustering formation was documented at ×100 magnification with a digital camera (Nikon D90) mounted to a phase-contrast microscope.

### Collagen contraction assays

HEp3 cells and their treatments were mixed with neutralized collagen solution (1 mg/mL in  $1 \times$  cell culture medium) at a concentration of 0.4 million cells/mL. The collagen/cell mixture was placed in the wells of a 24-well plate, allowed to solidify at 37°C, and cultured for 48 hours before analysis. The collagen was subsequently released from the wall of the culture well using a metal spatula and contraction of the collagen plug was documented 1 hour after release. The collagen plugs were documented at  $\times 100$  magnification with a digital camera (Nikon D90) mounted to a phase-contrast microscope.

### Patients and samples

Two retrospective cohorts of patients with prostate cancer were utilized in this study. The first cohort (cohort #1) of 99 cases underwent radical retropubic prostatectomy (RRP) between 1994 and 1998 at the London Health Sciences Centre with pathologic stage pT2–pT3 PCa (Supplementary Tables S1 and S2). A second cohort (cohort #2) of 38 cases was composed of diagnostic biopsy specimens from patients with prostate cancer at the same center who did not undergo RRP and developed metastatic disease during follow-up (Supplementary Table S3). Pathologic staging was re-evaluated according to TNM criteria (AJCC 2002). Patient characteristics and disease-related outcomes were obtained from a review of the medical records (Supplementary Tables S1–S3). This study obtained approval from an independent local Ethics Committee (UWO REB #15084E) and obtained the informed consent from all patients for the research use of their tissues.

### Immunohistochemistry

Formalin-fixed, paraffin-embedded tissue blocks were cut into 4  $\mu$ m sections and mounted onto positively charged glass slides. The tissue was deparaffinized and rehydrated using the xylene, graded ethanol, and water method. A two-step epitope retrieval was performed whereby tissue sections were boiled in the microwave in 10 mmol/L sodium citrate, 0.05% Tween 20 pH 6.0. The slides were then allowed to cool down, washed with PBS with 0.2% Triton-X (PBST), and incubated with pre-warmed pepsin (digest-all 3, Invitrogen) for 3 minutes. After washing with PBST, the specimens were stained using the UltraVision Detection System (Thermo Scientific). CD151 mAb 1A5 was diluted 1:800 in 1% BSA in PBS, CD151 mAb 11G5a (Abcam) was diluted 1:100 in 1% BSA in PBS, and  $\alpha 3\beta 1$  antibody P1B5 was diluted 1:250 in 1% BSA in PBS. Samples were then counterstained with hematoxylin and mounted with Cytoseal (Thermo Scientific). Negative controls were prepared using the identical treatment with omission of the primary antibody. Nonimmune mouse IgG was used as an additional negative control.

### CD151 expression analysis

CD151 expression in the RRP and biopsy cohorts detected by immunohistochemistry was categorized as negative (score = 0), weakly positive (score = 1), moderately positive (score = 2), or strongly positive (score = 3) independently by two pathologists who had no knowledge of the patient's clinical status. A consensus was reached where any discrepancy was identified.

To determine the statistical significance of mAb 1A5 immunoreactivity, specimens were divided into negative (score = 0) and positive (score = 1–3). CD151 protein expression analysis was performed in cancerous areas as well as benign tissue adjacent and distant from areas of tumor. Biochemical recurrence after RRP was defined as two consecutive prostate-specific antigen (PSA) measurements higher than 0.2 ng/mL. Bone metastasis was defined as the presence of metastatic lesions on a bone scan.

Profiling of CD151 mRNA expression in normal and prostate cancer tissue was accomplished using publicly available data obtained from the NCBI Gene Expression Omnibus (GEO) as well as The Cancer Genome Atlas (TCGA) via The cBio Cancer Genomics Portal (30). These included GDS2545 ( $n = 171$ ; ref. 31), GDS1439 ( $n = 19$ ; ref. 32), GSE6099 ( $n = 102$ ; ref. 33), and the prostate adenocarcinoma dataset from TCGA (34). Datasets were categorized according to their clinical diagnosis and analyzed by ANOVA with post-test analysis for linear trend. CD151 expression levels were extracted from publicly available expression dataset GDS3113 ( $n = 3$ /tissue; ref. 35) to demonstrate relative levels of CD151 expression in prostate compared with other tissues.

### Statistical analysis

Statistical analyses were performed using SAS version 9.2 (SAS Institute Inc.), SPSS 20 (IBM), and GraphPad Prism (GraphPad software). Experimental groups in migrations assays were compared with the control groups using a non-parametric Mann–Whitney test. The primary endpoint for cohort #1 is biochemical recurrence-free survival and the primary endpoint for cohort #2 is metastasis-free survival. Correlations between mAb 1A5 immunoreactivity and biochemical recurrence-free survival in malignant areas compared with benign areas were analyzed by McNemar  $\chi^2$  test. Kaplan–Meier plots were used to assess biochemical recurrence-free and metastasis-free survival. Group comparisons were made using the log-rank test. The Cox proportional hazard model was applied for multivariable analysis. In all statistical analyses, a two-sided  $P < 0.05$  was considered statistically significant. Graphical representation of statistical significance included \*, ( $P < 0.05$ ); \*\*, ( $P < 0.01$ ); and \*\*\*, ( $P < 0.001$ ).

### Image processing and analysis

Included images are representative of at least three replicate experiments. Fluorescent images are false-colored to represent specific labels. The brightness of images captured of *in vivo* experiments was uniformly adjusted for purposes of clarity. Where indicated, the images were cropped and scaled without any change in resolution. Quantitation of signal was performed on raw image files in Volocity Image Acquisition and Analysis Software (PerkinElmer) before creating the figures.

## Results

### CD151 clusters and accumulates at areas of cell–cell contact in response to mAb 1A5 binding

Given that tetraspanins facilitate macromolecular organization within cellular membranes, we hypothesized that the ability of anti-CD151 antibodies to influence migration

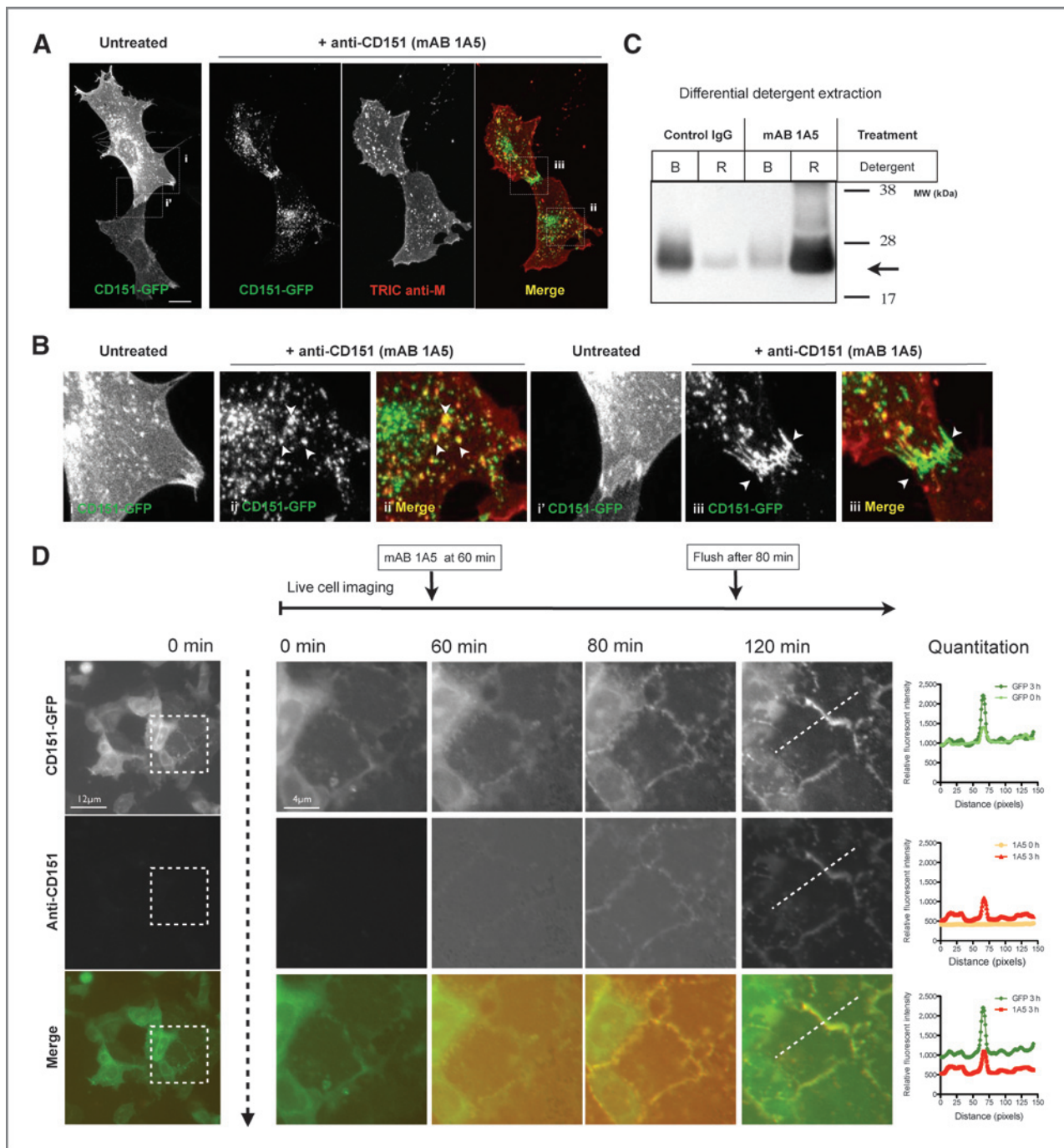


**Figure 1.** Cell surface clustering of CD151 in response to mAB 1A5. The cell surface distribution of CD151 was visualized by fluorescent microscopy in NIH3T3 cells after transfection with CD151-GFP and culture in the absence or presence of mAB 1A5 (2  $\mu$ g/mL) for 2 hours. **A**, CD151-GFP visualized in the absence (left) or presence of mAB 1A5 (right, 2  $\mu$ g/mL for 2 hours). Surface bound antibody was detected using TRIC-conjugated anti-mouse IgG post fixation. Insets in **A** emphasizing general cell surface (i and ii) versus areas of cell-cell contact (i' and iii) are magnified in **B**. **C**, surface CD151 was detected in sequential Brij99 and RIPA extractions with avidin-HRP after biotinylation of surface proteins and immunoprecipitating the tetraspanin from HEP3 cells cultured in the presence of a control IgG or mAB 1A5 for 24 hours. **D**, live-cell imaging was used to evaluate changes in CD151 distribution in response to mAB 1A5 binding. A549 cells transfected with CD151-GFP (green) were imaged every 5 minutes for 2 hours with the addition of Alexa 546-conjugated mAB 1A5 (red) added at  $t = 60$  minutes and flushed from the system at  $t = 80$  minutes.

involved changes in CD151 localization. This possibility was evaluated by analyzing changes in CD151 surface distribution in response to antibody binding (Fig. 1). NIH3T3 cells trans-

ected with human CD151-GFP exhibited a uniform surface distribution of CD151 when cultured at subconfluent densities (Fig. 1A and B, i/i'). Upon antibody binding, CD151-GFP

reorganized into punctate structures on the cell surface (Fig. 1A and B, ii) and accumulated at areas of cell–cell contact (Fig. 1A and B, iii). To confirm that antibody-bound CD151-GFP complexes were on the cell surface, a TRITC-conjugated secondary antibody was used to detect mAB 1A5 on the cell surface of intact cells fixed 2 hours after antibody treatment. Similar observations were made with HELA, HEP3, HT1080, and A549 cells. This data suggests that mAB 1A5 ligation of CD151 promotes the formation of macromolecular complexes (clustering) on the cell surface. Clustering of tetraspanins is known to cause a change in detergent solubility (1). To determine whether the antibody-mediated clustering induced a change in solubility, we performed cell surface biotinylation and differential detergent extraction of HEP3 cells treated with mAB 1A5 (Fig. 1C). Indeed, cell surface CD151 (biotinylated-CD151, arrow) became resistant to extraction by Brij99 and was solubilized by subsequent RIPA extraction. The increase in relative abundance of biotinylated CD151 in the RIPA re-extraction confirms that the clustered tetraspanin accumulated in detergent-resistant complexes on the cell surface.

When cell densities were sufficient to allow for cell–cell contact, antibody-binding induced clustering of CD151 at areas of cell–cell contact (Fig. 1B, iii) rather than at randomly distributed surface aggregates. To further assess the recruitment of CD151 to areas of cell contact, live-cell microscopy of densely cultured A549 cells expressing CD151-GFP was performed during the addition of Alexa 546-conjugated mAB 1A5 (Fig. 1D). A549 cells have intact cell–cell contacts where CD151 is readily visible. Addition of mAB 1A5 caused rapid accumulation of both labeled antibody and CD151-GFP in areas of cell–cell contact (Fig. 1D, "0 minute" vs. "120 minutes"). The accumulation of CD151 at areas of cell–cell contact was quantified by mapping pixel intensity from time 0 to 120 minutes in the GFP channel (CD151-GFP) and the Alexa 546 channel across a reference line. Although A549 cells have well established cell–cell contacts, similar observations were made for epithelial-derived cancer lines that lack stable cell–cell contacts such as the HNSCC HEP3 during *in vitro* culture (Supplementary Movie S1) and *in vivo* tumor growth (Supplementary Fig. S1). Thus, clustered CD151 accumulated at areas of cell–cell contact in all models and experimental settings.

#### Antibody-induced clustering promotes an adhesive phenotype

We previously observed that mAB 1A5 prevents detachment at the rear of migrating cells thereby inhibiting tumor cell migration and metastasis *in vivo* (6). Evaluation of HEP3 migration at increasing concentrations of mAB 1A5 demonstrated a dose-dependent inhibition of migration *in vitro* (Fig. 2A) and *in vivo* (Fig. 2B). In the presence of control antibody, GFP-expressing HEP3 form metastatic colonies composed of widely spaced individual cells that are disseminating freely into the surrounding tissue. In contrast, treatment with mAB 1A5 limited cell motility, resulting in the formation of compact colonies at concentrations as low as 0.5  $\mu$ g antibody per animal (Fig. 2B, top right). The ability to immobilize tumor cells *in vivo* at such low antibody concentrations together with previous

observed inhibition of detachment (6) suggests that the tetraspanin clustering mediates a gain of adhesive function.

To confirm that CD151 clustering in response to mAB 1A5 induces adhesion, we evaluated a range of cellular behaviors dependent upon adhesion, including collagen contraction, fibronectin fibrillogenesis, platelet aggregation, and clustering of nonadherent cells. Collagen contraction assays performed in the presence of mAB 1A5 demonstrated that CD151 clustering promotes collagen contraction when compared with cells treated with the control antibody (Fig. 2C). This is in contrast with the inhibition of collagen contraction by agents that inhibit matrix remodeling by MMPs (GM6001) or block integrin-mediated adhesion to collagen (anti- $\alpha$ 2 $\beta$ 1 integrin). Fibronectin fibrillogenesis, an integrin-dependent process (36), was evaluated in HT1080 cells. These cells exhibit very limited fibril assembly during routine culture, but treatment with mAB 1A5 resulted in the formation of visible fibrils compared with the control IgG-treated cells (Fig. 2D). Platelet aggregation is an integrin-dependent process stimulated by collagen binding or thrombin-mediated protease activated receptors (PAR; ref. 37). Platelets express an abundance of CD151 where it contributes functionally to platelet aggregation via  $\alpha$ IIB $\beta$ 3 (15). Treatment with mAB 1A5 stimulated dose-dependent platelet aggregation, which could be prevented with integrin-blocking cyclic RGDS peptide, suggesting ligand-specific adhesion through integrins (Fig. 2E). Finally, antibody binding promoted clustering of lymphoma (U937) and leukemia (Jurkat) cells (Supplementary Fig. S2A and S2B). Staining of suspended cells with mAB 1A5 after fixation demonstrates uniform surface distribution of CD151 (post-fixation, Supplementary Fig. S2B). In contrast, treatment of the cells with mAB 1A5 before fixation induced clustering of the cells and resulted in accumulation of the antibody-CD151 complex at areas of cell–cell contact similar to what was observed for adherent cells (Fig. 1). These observations consistently demonstrate the clustering of CD151 to promote cell adhesion.

#### MAB1A5 binds CD151 not associated with integrin $\alpha$ 3 (CD151<sup>free</sup>)

The ability of CD151 to contribute to adhesion and motility on laminin through direct interaction with the laminin-binding integrins  $\alpha$ 3 $\beta$ 1 and  $\alpha$ 6 $\beta$ 1 is well established (10, 11). However, much of the adhesive behavior described above did not involve laminin and adhesion to collagen, assembly of fibronectin, and the aggregation of platelets (Fig. 2C–E) does not involve integrins that contain the  $\alpha$ 3 or  $\alpha$ 6 subunits. These observations suggest that CD151 clustering and biologic activity in response to mAB 1A5 was independent of its association with laminin-binding integrins. Yamada and colleagues (19) demonstrated that several CD151 antibodies recognize the integrin-binding domain of CD151 and only bind CD151 that is dissociated from its integrin partners (CD151<sup>free</sup>). Together, these observations suggest that an integrin-independent mechanism might be involved in the regulation of adhesion by CD151.

To determine whether mAB 1A5 selectively recognizes CD151<sup>free</sup> versus CD151<sup>ITGA</sup>, its ability to coimmunoprecipitate an integrin partner was evaluated. A comparison was made

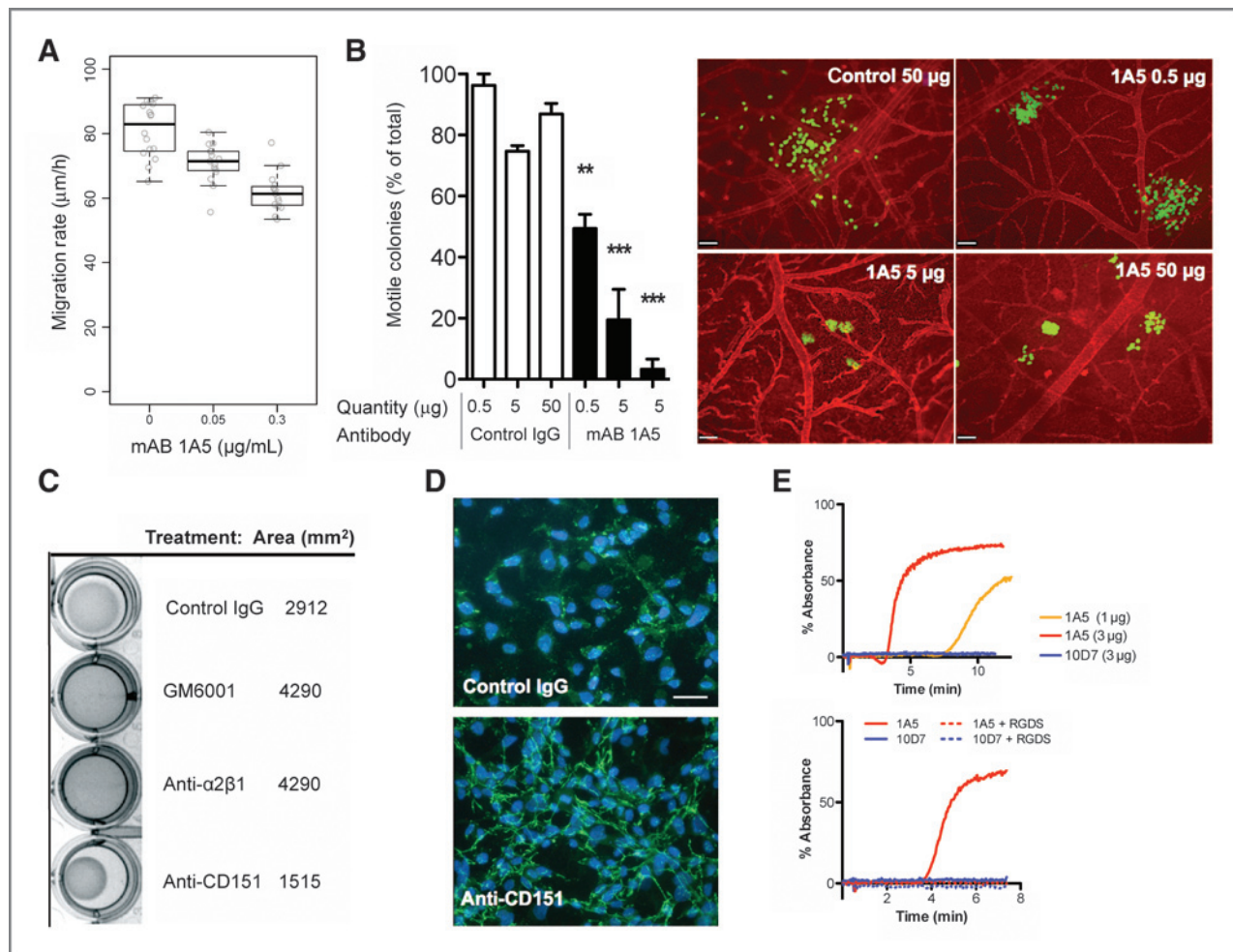


**Figure 2.** Antibody-mediated clustering promotes an adhesive phenotype. **A**, dose-dependent inhibition of HEP3 cell migration in response to mAB 1A5 using an *in vitro* wound healing assay. **B**, dose-dependent inhibition of HEP3 cell migration in the CAM of chick embryos in response to mAB 1A5 treatment. **C**, collagen contraction by HT1080 cells in response to mAB 1A5 when compared with control IgG, inhibition of MMP activity (GM6001), and blocking of collagen binding ( $\alpha 2\beta 1$ ). **D**, fibronectin fibrillogenesis in response to mAB 1A5 or control IgG treatment as detected by immunofluorescent staining of fibronectin fibrils. **E**, platelet aggregation in response to mAB 1A5 treatment in the presence or absence of RGDS peptides to block integrin-mediated adhesions.

with an antibody specific for the integrin-binding domain that cannot precipitate the integrins (8C3) and an antibody that binds outside this domain and readily precipitates the integrin partners (11G5A; ref. 19). Since our principle tumor model (HEP3) is nearly devoid of  $\alpha 6$ , we evaluated integrin interactions primarily by monitoring  $\alpha 3$ . Immunoprecipitates of CD151 from TX-100 lysates of A549 (Fig. 3A) and HEP3 cells (Supplementary Fig. S3) were evaluated for the presence of  $\alpha 3$  by immunoblotting. The integrin subunit  $\alpha 3$  coimmunoprecipitated with CD151 bound by mAB 11G5A but not 1A5 or 8C3 (Fig. 3A). Similar observations were made in immunoprecipitations from HEP3 cells (Supplementary Fig. S3). To determine whether mAB 1A5 bound the CD151/ $\alpha 3\beta 1$  complex in intact cells, we treated A549 cells overnight with mAB 1A5 (2 µg/mL) and lysed the cultures in Triton X-100 lysis buffer after removing all unbound antibody. The cell lysate was immunodepleted with protein-G sepharose beads in three sequential incubations and the presence of  $\alpha 3$  and CD151 was subsequently evaluated in both the bound and unbound fractions. Antibody-

bound CD151 was removed in the first round of immunodepletion, whereas  $\alpha 3$  remained in the unbound fraction. To confirm that the CD151 that remained in the unbound fraction remained associated with  $\alpha 3$ , we immunoprecipitated the integrin with mAB P1B5 and evaluated both bound and unbound fractions for  $\alpha 3$  and CD151 (Fig. 3C). The majority of CD151 in the lysate coimmunoprecipitated with  $\alpha 3$ . Since mAB 1A5 failed to coprecipitate  $\alpha 3$  and the integrin remained associated with CD151 not bound by the antibody, we conclude that mAB 1A5 only binds CD151 that is not engaged with  $\alpha 3$ .

#### mAB 1A5 specifically recognizes the integrin-binding domain of CD151

The integrin-binding domain of CD151 includes the <sup>194</sup>QRD<sup>196</sup> sequence of its large extracellular loop (11). Anti-CD151 antibodies that are unable to precipitate the CD151/ $\alpha 3\beta 1$  complex frequently bind this domain (38). Yamada and colleagues used two-color flow cytometry to map epitope-binding of human-specific anti-CD151 antibodies according to

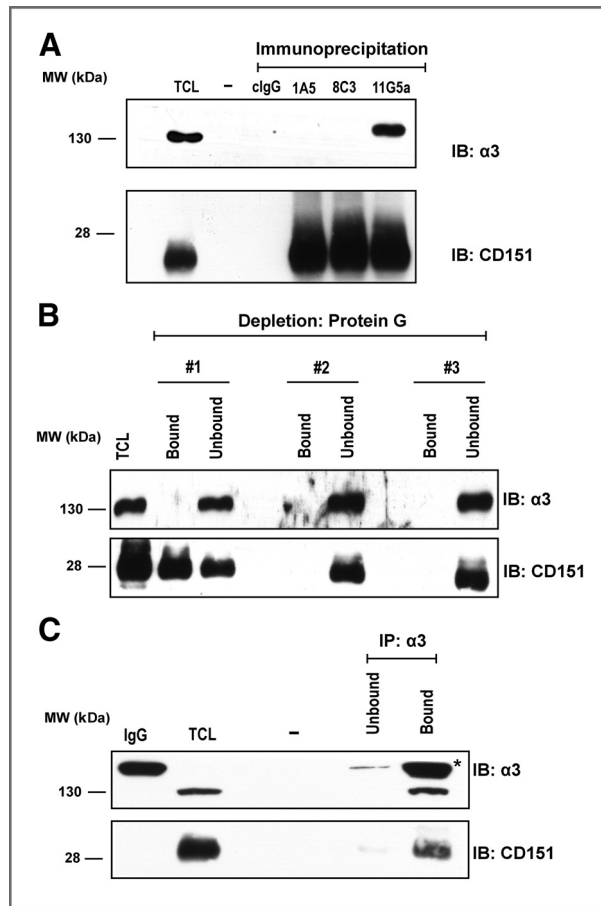


**Figure 3.** MAB 1A5 binds to CD151 not engaged with integrin  $\alpha 3$ . **A**, immunoblot of  $\alpha 3$  and CD151 after immunoprecipitation of the tetraspanin from A549 cell lysates (Triton X-100) using non-specific mouse antibody (clgG) and three distinct antibodies against CD151 (1A5, 8C3, and 11G5a). **B**, A549 cells were cultured in the presence of mAB 1A5 for 24 hours. Cell lysates were generated with Triton X-100 and antibody bound CD151 was depleted from the lysate in three sequential incubations with immobilized Protein-G. Bound and unbound fractions were analyzed for  $\alpha 3$  and CD151 by immunoblotting. **C**, the integrin subunit  $\alpha 3$  was immunoprecipitated from the unbound fraction of the 3rd depletion from **B** with anti- $\alpha 3$  (P1B5) and this sample was evaluated for the presence of  $\alpha 3$  and coprecipitated CD151 by immunoblotting. TCL, total cell lysate; IgG refers to normal mouse included as a reference for the IgG band (\*).

their reactivity with CD151 mutants, in which 12 residues across the large extracellular loop of the human protein were substituted with their mouse counterpart (Supplementary Fig. S4A and S4B; ref. 19). We implemented a similar approach to determine which residues of CD151 are involved in antigen recognition by mAB 1A5. GFP fusions of the human-mouse CD151 substitution mutants were transiently expressed in NIH3T3 cells and subsequently stained with anti-CD151 antibody. Flow cytometry was used to detect cells positive for both GFP and Alexa 647 (Fig. 4). This analysis was performed for all substitution mutants (Supplementary Fig. S4D). mAB 1A5 bound every substitution mutant except the <sup>194</sup>QRD<sup>196</sup> mutant, in which the glutamine at position 194 is mutated to a lysine. This analysis was done in parallel with two antibodies previ-

ously shown to interact with this domain (8C3 and 14A2.H1) and contrasted to an antibody known not to bind to this region (11G5A, Fig. 4). These observations confirm that mAB 1A5 binds CD151 through the integrin-binding domain containing the <sup>194</sup>QRD<sup>196</sup> sequence.

#### Antibodies that recognize the integrin-binding domain of CD151 can inhibit tumor cell motility *in vivo*

Yamada and colleagues (19) stratified anti-CD151 antibodies according to their epitope specificity. mAB 1A5 belongs to "group I," which contains antibodies that specifically recognize CD151<sup>free</sup> because they bind the integrin-binding domain and fail to immunoprecipitate  $\alpha 3$ . Since mAB 8C3 and 1A5 share epitope specificity, we hypothesized that they might also share the ability to cluster the tetraspanin at areas of cell-cell contact. Live-cell imaging of A549 cells expressing CD151-GFP confirmed that mAB 8C3 but not 11G5A can cluster the tetraspanin (Supplementary Fig. S5). Since antibodies in "Group I" share both domain-specificity and the ability to cluster CD151, we explored the possibility that these antibodies specific for CD151<sup>free</sup> can control tumor cell migration. To achieve this, HEP3-GFP cells injected intravenously into chick embryos were treated with antibodies specific for CD151<sup>free</sup> (8C3, 14A2.H1, and 1A5) and an antibody that binds outside this domain (11G5A) or a control antibody (Fig. 5A). Metastatic colonies were allowed to form for 3 days before their morphology was documented and the number of colonies with a motile phenotype was quantified (Fig. 5B). At 0.5 to 5  $\mu$ g/animal, only mAB 1A5 inhibited tumor cell motility *in vivo*. However, at 20  $\mu$ g/animal, tumor cell motility was inhibited by 8C3 and 14A2.H1 but not 11G5A or the control antibody. These data demonstrate that antibodies specific for CD151<sup>free</sup> are capable of inhibiting tumor cell migration by clustering CD151 not associated with integrins.

#### Tumor cell immobilization in response to CD151 clustering requires PKC $\alpha$ but not integrin $\alpha 3$

To determine whether  $\alpha 3$  is required for the immobilization mediated by CD151, *in vivo* migration assays were performed following  $\alpha 3$  knockdown. HEP3 cells were transfected with control or  $\alpha 3$ -specific siRNA and a 90% or more reduction in  $\alpha 3$  expression after siRNA delivery was confirmed by immunoblotting (Fig. 6A). HEP3 cells bearing control or  $\alpha 3$ -specific siRNA were subsequently injected into chick embryos and allowed to form metastatic colonies in the presence of mAB 1A5 or a control antibody (29-7). Knockdown of  $\alpha 3$  did not impair the migration of tumor cells as evidenced by the absence of colonies with an immobilized phenotype (Fig. 6B and C). Moreover, in the presence of mAB 1A5, both HEP3 control- and  $\alpha 3$ -siRNA-transfected cells form compact colonies demonstrating that the absence of  $\alpha 3$  does not alter the ability of CD151 clustering to inhibit motility and colonization *in vivo*. PKC $\alpha$  is a known signaling partner of CD151. To determine whether PKC $\alpha$  is required for the inhibition of tumor cell motility upon CD151 clustering, *in vivo* migration assays were performed following PKC $\alpha$  knockdown (Fig. 6). The knockdown of PKC $\alpha$  did not affect tumor cell motility but

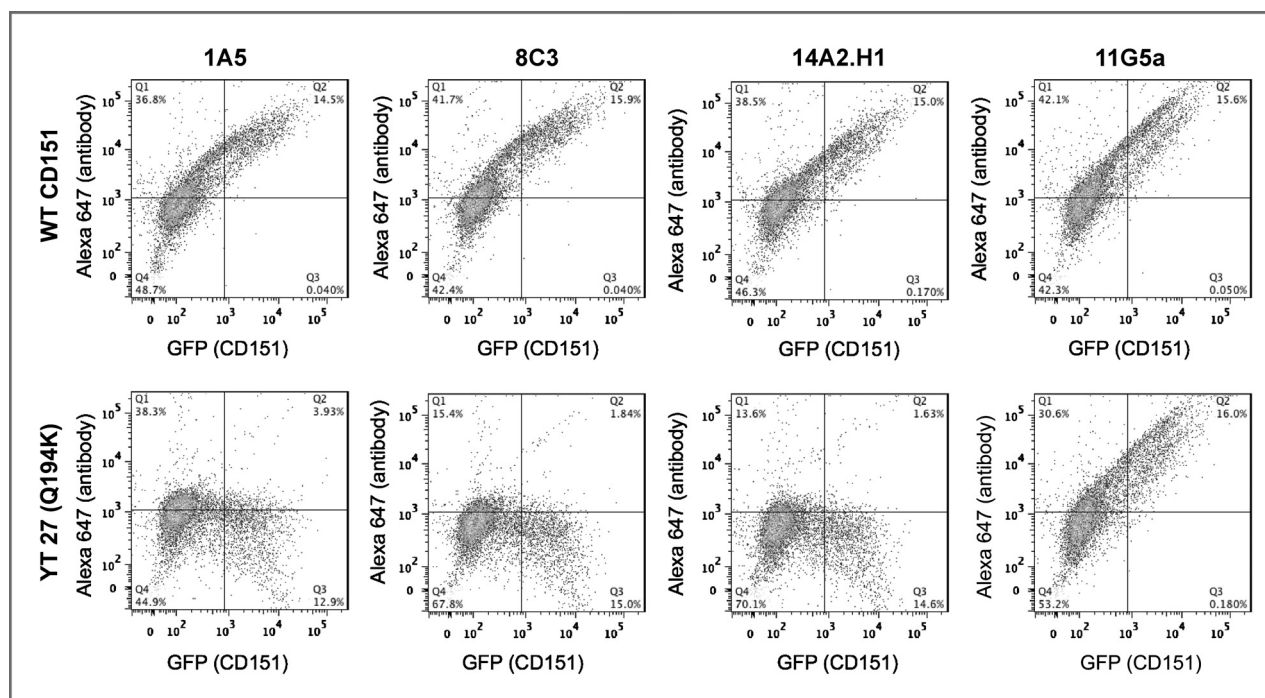


Figure 4. mAB 1A5 recognizes the integrin-binding domain of CD151. Two-color flow cytometry of the CD151 human/mouse substitution mutants was used to evaluate what epitope on CD151 is required for mAB 1A5 binding. NIH3T3 cells were transiently transfected with WT or mutant CD151-GFP constructs. Transgene expression was detected using GFP while antibody binding was detected using an Alexa 647-conjugate anti-mouse IgG. A comparison is made between WT CD151 and the Y27 (Q194K) mutant, which disrupts binding with the  $\alpha 3$  integrin subunit. MAB 1A5 is compared with two antibodies known for their inability to bind this mutant (8C3 and 14A2.H1) and one antibody whose binding is unaffected by this mutation (11G5A). A loss of antibody binding is represented by a decrease in the percentage of GFP and Alexa 647 double positive cells in quadrant (Q2). The full panel of human/mouse substitution mutants is shown in Supplementary Fig. S4.

did prevent immobilization in response to mAB 1A5-induced clustering of CD151.

#### The integrin-binding domain of CD151 is detectable in prostate cancer and corresponds with poor patient outcome

Antibodies specific for integrin-binding domain of CD151 define a subpopulation of this tetraspanin (CD151<sup>free</sup>) that is distinct from the tetraspanin bound to its integrin partner (CD151<sup>ITGA</sup>). The immobilization of tumor cells through clustering of CD151<sup>free</sup> (Figs. 5 and 6) and the subsequent inhibition of metastasis (6) demonstrates that CD151<sup>free</sup> may be relevant in the malignant progression of cancer. Recent work demonstrated a specific role for CD151 in the progression of prostate cancer (39). We hypothesized that detection of CD151<sup>free</sup> is altered during tumor progression and correlates with patient outcome. This relationship was evaluated in prostate cancer by comparing the detection of CD151<sup>free</sup> to biochemical recurrence (for patients who underwent RRP: cohort #1,  $N = 99$ ) or metastasis (for patients who did not undergo RRP: cohort #2,  $N = 38$ ). See Supplementary Tables S1–S3 for patient information.

Histologic detection with the mAB 11G5A (which binds both CD151<sup>ITGA</sup> and CD151<sup>free</sup>) demonstrates abundant expression of CD151 in both normal and malignant prostate tissues. Conversely, mAB 1A5 (which binds only CD151<sup>free</sup>) exhibited weak staining of normal prostate glands but

elevated detection of CD151<sup>free</sup> in tissue from prostate cancers (Fig. 7A). CD151 gene expression is relatively abundant in normal adult prostate tissue (Supplementary Fig. S6A). An analysis of CD151 mRNA expression in prostate cancer studies available through The Cancer Genome Atlas (TCGA; CD151, Fig. 6B) and NCBI GEO (Supplementary Fig. S6B–S6D) revealed no significant changes in *CD151* gene expression. This observation is in accordance with our histologic assessment of CD151 protein detection with 11G5A (Fig. 7A). In contrast, 55% of the 216 patients with prostate adenocarcinoma analyzed in the TCGA exhibited reduced expression of integrin  $\alpha 3$  (ITGA3, Fig. 6B). This observation suggested that the appearance of CD151<sup>free</sup> might coincide with reduced expression of integrin  $\alpha 3$ . Indeed, paired histologic analysis of advanced prostate cancer tumors reveals that CD151 is readily detected in the tumor tissue, adjacent normal, and distant normal tissue. In contrast, integrin  $\alpha 3$  expression is reduced in the tumor relative to normal tissue and CD151<sup>free</sup> is detectable only in the tumor (Fig. 7C). Independent histologic evaluation of integrin  $\alpha 3$  and CD151 available through the Human Protein Atlas (40) confirms reduced expression of the integrin in tumor tissue compared with normal tissue not only in prostate cancer (Fig. 7D quantified in E) but also in cancers of the breast, colon, and kidney (Fig. 7D).

To evaluate the correlation of CD151<sup>free</sup> with patient outcome in prostate cancer, we compared the levels of

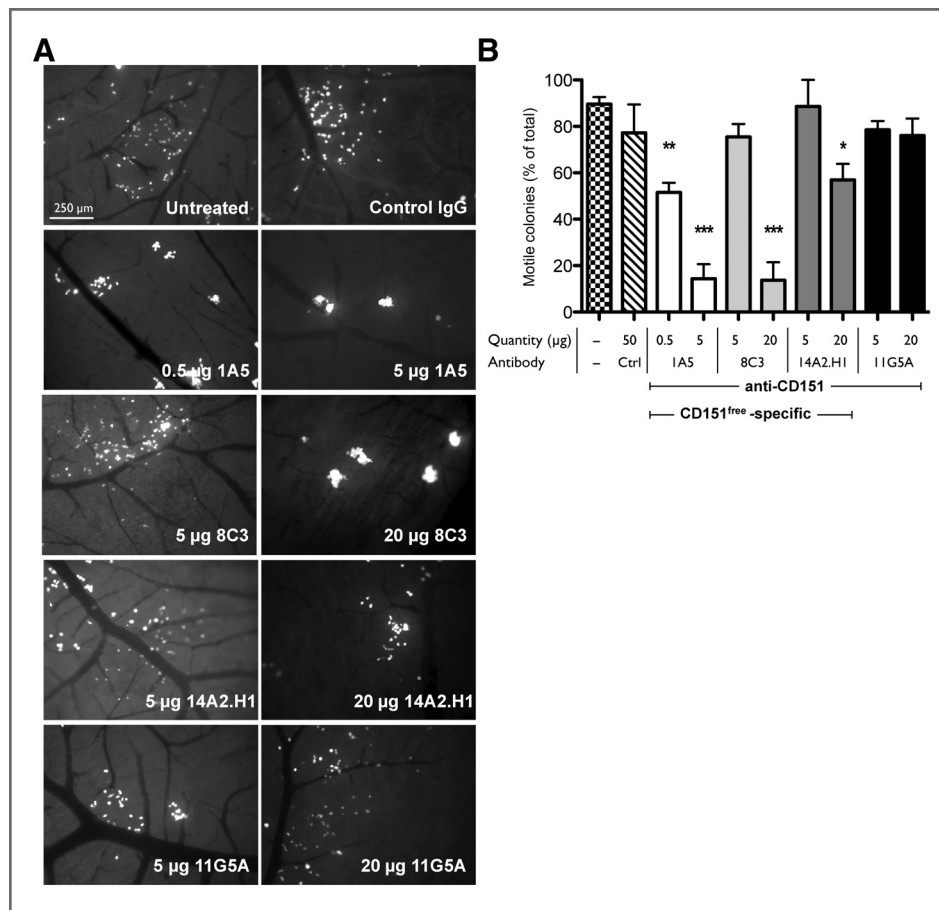


**Figure 5.** Clustering of CD151 through antibodies specific for the integrin-binding domain inhibits tumor cell motility *in vivo*. Changes in tumor cell motility in response to anti-CD151 antibodies were determined by analyzing the formation of metastatic colonies in the chorioallantoic membrane. A, the inhibition of tumor cell dissemination in the presence or absence of anti-CD151 antibodies (1A5, 8C3, 14A2.H1, and 11G5A) was compared with the dissemination in the absence of tumor-targeting antibodies (untreated) or a control IgG. Images were taken after 4 days of treatment with 0.5, 5, or 20 μg or antibody (A) and the number of colonies with motile tumor cells were quantified (B).  $N \geq 5$  with experiments performed in duplicate.

CD151<sup>free</sup> to biochemical recurrence (for patients who underwent RRP: cohort #1,  $N = 99$ ) or metastasis (for patients who did not undergo RRP: cohort #2,  $N = 38$ ). See Supplementary Tables S1–S3 for cohort descriptions. First, we dichotomized patients that underwent RRP (cohort #1) based on mAB 1A5 staining (positive vs. negative). CD151<sup>free</sup> staining on benign tissue adjacent to the tumor (Supplementary Fig. S8A) and normal tissue distant from the tumor (Supplementary Fig. S8B) failed to demonstrate an association with biochemical recurrence. In contrast, detection of CD151<sup>free</sup> (mAB 1A5 positive) in tumor tissue corresponded to a significantly reduced time-to-biochemical recurrence compared with tumor tissue with no detectable levels of CD151<sup>free</sup> (mAB 1A5 negative, Fig. 7F; mean survival = 10.3 vs. 13.5; log-rank;  $P = 0.023$ ). Moreover, the detection of CD151<sup>free</sup> further stratified patients that were already stratified by high ( $\geq 8$ ) and low ( $< 8$ ) baseline PSA levels in regards to biochemical recurrence (Fig. 7G). Biochemical recurrence-free survival is reduced in patients that are singly positive for either CD151<sup>free</sup> or high PSA compared with those negative for both (mean survival = 11.6 and 12.3 years vs. no recurrence; log-rank;  $P = 0.068$ ). Furthermore, singly positive patients have significantly greater biochemical recurrence-free survival compared with patients that are double positive (mean survival = 11.6 and 12.3 years vs. 9.1

years; log-rank;  $P = 0.017$ ). Most importantly, in patients with high PSA, CD151<sup>free</sup> (positive vs. negative) is an independent predictor of biochemical recurrence-free survival after adjusting for tumor stage (adjusted HR = 13.5; 95% confidence interval, 1.2–148.1;  $P = 0.033$ ). To determine if the presence of CD151<sup>free</sup> in the primary tumor could be indicative of future metastasis, we evaluated biopsy specimens from prostate cancer patients that did not undergo RRP and eventually developed metastasis (cohort #2). Patients were dichotomized according to absence/presence of mAB 1A5 staining and its relation to metastasis-free survival was visualized using Kaplan–Meier analysis (Fig. 7H). Patients with mAB 1A5-positive biopsies at time of diagnosis exhibited a greatly reduced metastasis-free survival (mean survival = 3.7 vs. 12.7; log rank  $P = 0.001$ ).

These observations indicate that CD151<sup>free</sup> is evident only in tumor tissues where its appearance coincides with reduced integrin  $\alpha 3$  expression and its detection is an independent negative predictor of biochemical-free as well as metastasis-free survival.

## Discussion

The tetraspanin CD151 is an established regulator of cell adhesion, migration, and tumor cell metastasis (5, 20, 39, 41).

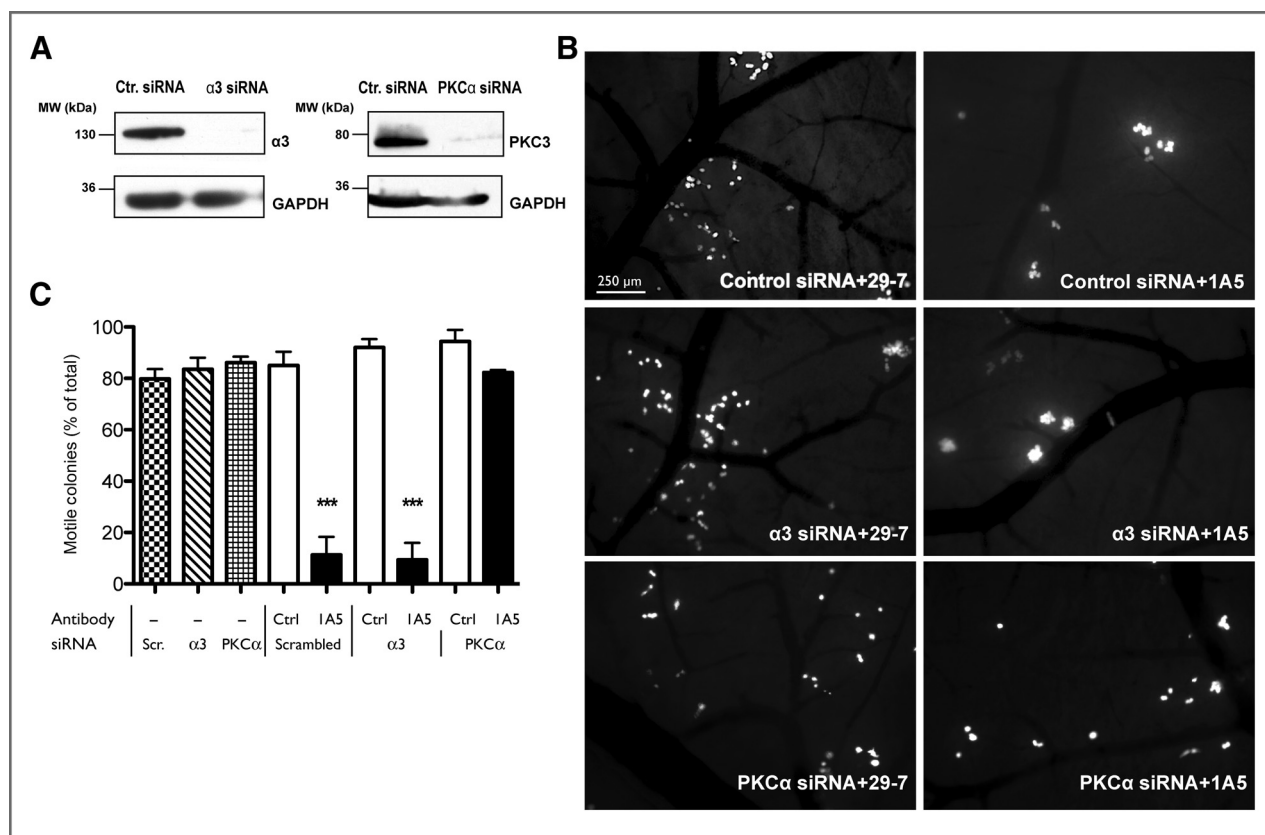


**Figure 6.** PKC $\alpha$  but not integrin  $\alpha 3$  is required for the regulation of motility through CD151<sup>free</sup>. A, immunoblotting of Triton-X 100 lysates from HEp3 cells transfected with the control, integrin  $\alpha 3$ -specific, or PKC $\alpha$ -specific siRNA to evaluate the efficacy of target gene knockdown. GAPDH is included as a loading control. B, the analysis of tumor cell motility *in vivo* after delivery of control, integrin  $\alpha 3$  or PKC $\alpha$  siRNA. Tumor-bearing embryos were treated with control IgG or mAB 1A5 (5  $\mu$ g) 1 day after tumor cell injection. Images of metastatic colonies were taken 2 days after antibody injection. The immobilization of tumor cells in response to mAB 1A5 was quantified in C.  $N \geq 5$  with experiments performed in triplicate.

Its interactions with the integrin subunits  $\alpha 3$  and  $\alpha 6$  have been shown to be important for adhesion, migration, and morphogenesis on laminin (11–13, 18, 42). However, using immunoprecipitation and flow cytometry, we demonstrate that there is a subpopulation of CD151 on the surface of tumor cells that is not associated with its integrin partner (CD151<sup>free</sup>). This population of CD151<sup>free</sup> can be detected with antibodies specific for the integrin-binding domain of CD151, including mAB 1A5, 8C3, and 14A2.H1.

We previously demonstrated that anti-CD151 mAB 1A5 potently inhibits tumor cell migration and metastasis (6) by preventing deadhesion at the rear of the cell. The inhibition of motility required a bivalent antibody, suggesting that mAB 1A5 could mediate its activity by clustering the tetraspanin. Indeed, mAB 1A5, along with other antibodies specific for the integrin-binding domain of CD151 cluster the tetraspanin. Clustering of CD151<sup>free</sup> promotes cell adhesion and results in tumor cell immobilization, enhanced collagen contraction, greater fibronectin fibrillogenesis, improved platelet aggregation, and elevated cell–cell adhesion. Although many of these activities are integrin-dependent, they do not involve adhesion to laminin nor association with the laminin-binding integrins that are established integrin partners of CD151. Indeed, the immobilization of tumor cells

in response to the clustering of CD151<sup>free</sup> does not require  $\alpha 3$  expression (Fig. 6). We have previously demonstrated that the loss of CD151 does not lead to tumor cell immobilization (6), thus the inhibition of tumor cell motility associated with the clustering of CD151<sup>free</sup> is likely a distinct mechanism for the control of cellular adhesion and migration.

These observations raise a number of questions, including (i) what mechanism creates CD151<sup>free</sup>? (ii) does CD151<sup>free</sup> occur in normal tissue? (iii) is the mechanism by which CD151<sup>free</sup> controls motility distinct from the mechanism of integrin-associated CD151?, and (iv) is CD151<sup>free</sup> a tumor promoter? While fully answering these questions will require further investigation, significant insight is available from these and published studies. CD151<sup>free</sup> could become available when the stoichiometric balance with its integrin partners is altered. This alteration is evident when the expression of integrin  $\alpha 3$  is significantly reduced in tumor relative to normal tissue (Fig. 7) but could also occur when CD151 expression is upregulated as reported for hepatic carcinomas (43). However, CD151<sup>free</sup> is also likely to occur in normal tissues when expression of the laminin-binding integrins is reduced or absent. This is evident in cardiac tissue that exhibits little  $\alpha 3$  and  $\alpha 6$  expression but an



abundance of CD151 that is detectable by antibodies specific to the integrin-binding epitope (11B1, 14A2.H1; ref. 22). Even more evident is the presence of CD151<sup>free</sup> in the bone marrow, circulating hematopoietic cells, and platelets where the laminin-binding integrins have low expression and the surface expression of CD151<sup>free</sup> is readily detectable with any of the antibodies specific for integrin-binding epitope. The ability of mAB 1A5 to promote adhesion in platelets and suspended hematopoietic cell lines (Fig. 1) is perhaps the first and most obvious evidence that CD151<sup>free</sup> can control an adhesive mechanism distinct from the laminin-binding integrins. The universality of CD151 clustering via the integrin-binding epitope is confirmed with additional antibodies with epitope specificity similar to mAB 1A5 (Fig. 5). The extent to which individual CD151 antibodies inhibited migration varied. These differences are likely due to variations in their individual affinity and ability to cluster CD151. There are additional anti-CD151 antibodies not tested here. TS151r has been reported to displace integrin partners from CD151 (24) and subsequently promote migration of epithelial cells. Although we only observed inhibition of migration in response to anti-CD151 antibodies, Chometon and colleagues evaluated the migration of a relatively benign cell line on laminin (24). Reducing the laminin binding would likely accelerate migration. Future studies will determine evaluate the ability of the antibodies TS151r and TS151 to promote CD151 and alter migration of metastatic cell lines on non-laminin substrates.

The ability of CD151<sup>free</sup> clustering to inhibit tumor cell migration after the knockdown of  $\alpha 3$  (Fig. 6) suggests that CD151<sup>free</sup> can also regulate adhesion and migration of epithelial-derived tumor cells through a mechanism independent of laminin-binding integrins. A preliminary evaluation of the CD151 signaling mechanisms revealed that neither Rac nor Rho activity was altered upon CD151<sup>free</sup> clustering. However, the canonical signaling partner of CD151, PKC $\alpha$ , was required for CD151<sup>free</sup> clustering to inhibit tumor cell motility. Although PKC $\alpha$  is generally thought of as a promoter of migration, PKC $\alpha$  was identified as an inhibitor of cell migration by the Brugge laboratory during an *in vitro* screening assay of normal epithelial migration (44).

We hypothesize that the distinct mechanisms by which CD151 can regulate cell adhesion and migration are determined primarily by the nature of the associated partner and the cellular context in which they function. In the context of a transformed cancer cell, the CD151-integrin-laminin axis (CD151<sup>ITGA</sup>; refs. 13, 14) participates in promoting tumor cell invasion and metastasis (10, 11, 41, 42, 45), whereas in normal, quiescent epithelia, the association of CD151 with the laminin-binding integrins is required for cohesion and (non-motile) epithelial integrity (16, 46). Clearly, the loss of CD151 diminishes both normal epithelial integrity and cancer metastasis, suggesting that both phenomena, which are on opposing ends of the motility spectrum, utilize the adhesion facilitated by CD151. Conversely, CD151<sup>free</sup> present on migratory/metastatic cells as well as nonadherent cells (hemopoietic cells and platelets) can initiate/promote adhesion, resulting in aggregation (platelets, Fig. 1; nonadherent cells, Supplementary

Fig. S2) or inhibition of migration (tumor cells, Fig. 1; ref. 6) when clustered.

Cell motility is directly linked to dynamic cycling of adhesion/deadhesion (47). Firm adhesion as seen in normal epithelial cells on laminin-containing basement membranes limits cell motility but promotes epithelial integrity (47, 48). Although the detection of CD151<sup>free</sup> correlates with metastasis, it is not clear that CD151<sup>free</sup> contributes directly to metastatic progression. CD151<sup>free</sup> appears to be created upon the loss of  $\alpha 3$  and this coincides with increased metastatic behavior. The genetic ablation of CD151 clearly diminishes metastasis (5, 14, 39) demonstrating that CD151 supports metastasis. In the instance of CD151<sup>free</sup>, it remains to be determined whether metastasis is promoted by the loss of  $\alpha 3$  or the gain of integrin-free CD151. However, it is clear that clustering of CD151<sup>free</sup> promotes adhesion and inhibits migration. Although the molecular mechanism by CD151<sup>free</sup> might control motility is currently unknown, uncoupling CD151 from the laminin-binding integrins is likely to promote a less adhesive, more motile phenotype. This is not only supported by the reduction of integrin  $\alpha 3$  in tumor cells but also the loss of the integrin during *in vitro* selection for matrix invasion (49) and an increase in metastasis after targeted knockdown of integrin  $\alpha 3$  (50). Considering the immobility of firmly anchored cells in normal epithelia, the creation of CD151<sup>free</sup> during tumorigenesis is a simple mechanism to promote motility. Furthermore, CD151<sup>free</sup> can be engaged (clustered) to stimulate adhesion (Fig. 2 and Supplementary Fig. S2; ref. 6), suggesting that the creation of CD151<sup>free</sup> would bias tumor cells towards a more dynamic cycling of adhesion in favor of migration and thereby promote tumor metastasis. What remains to be determined is the identity of partners that control the switch of CD151<sup>free</sup> to its adhesion-promoting state.

In conclusion, our findings demonstrate that a subpopulation of CD151 exists on the surface of tumor cells that is not associated with integrin partners (CD151<sup>free</sup>) that regulate tumor cell migration. Clinical correlation of CD151<sup>free</sup> with prostate cancer progression demonstrates that it has independent prognostic value and suggests that this tetraspanin subpopulation may contribute to the disease and could be used to predict cancer progression.

#### Disclosure of Potential Conflicts of Interest

No potential conflicts of interest were disclosed.

#### Authors' Contributions

**Conception and design:** T.D. Palmer, C.H. Martinez, V. Chalasani, J.D. Lewis, A. Zijlstra

**Development of methodology:** T.D. Palmer, C.H. Martinez, C. Vasquez, C. Jones-Paris

**Acquisition of data (provided animals, acquired and managed patients, provided facilities, etc.):** T.D. Palmer, C.H. Martinez, C. Vasquez, K. Hebron, C. Jones-Paris, S.M. Chan, V. Chalasani, A.K. Williams, J.L. Chin, G.A. Giannico, T. Ketova

**Analysis and interpretation of data (e.g., statistical analysis, biostatistics, computational analysis):** T.D. Palmer, C.H. Martinez, K. Hebron, S.A. Arnold, J.L. Chin, J.D. Lewis, A. Zijlstra

**Writing, review, and/or revision of the manuscript:** T.D. Palmer, C.H. Martinez, C. Vasquez, S.A. Arnold, V. Chalasani, J.D. Lewis, A. Zijlstra

**Administrative, technical, or material support (i.e., reporting or organizing data, constructing databases):** T.D. Palmer, C.H. Martinez, C. Vasquez, T. Ketova, J.D. Lewis, A. Zijlstra

**Study supervision:** C.H. Martinez, J.A. Gomez-Lemus, J.D. Lewis, A. Zijlstra

## Acknowledgments

The authors thank Amber Ablack and Carl Postenka for their valuable technical support, Kristin Kain for editorial input, and Larry Stitt for the statistical analysis. Fertilized eggs were kindly provided by Tyson Food Inc.

## Grant Support

This study was supported by CA143081 and CA120711 from the NIH to A. Zijlstra and Motorcycle Ride for Dad as well as Canadian Cancer Society Research Institute Grant #700537 (J.D. Lewis). J.D. Lewis holds the Frank and Carla Sojonyk Chair in Prostate Cancer Research funded by the Alberta

Cancer Foundation. NIH support was provided to T.D. Palmer under CA136228 and GM008554, K.E. Hebron under CA009592, and C. Jones-Paris under GM008554.

The costs of publication of this article were defrayed in part by the payment of page charges. This article must therefore be hereby marked *advertisement* in accordance with 18 U.S.C. Section 1734 solely to indicate this fact.

Received January 30, 2013; revised September 27, 2013; accepted October 22, 2013; published OnlineFirst November 12, 2013.

## References

- Hemler ME. Tetraspanin functions and associated microdomains. *Nat Rev Mol Cell Biol* 2005;6:801–11.
- Zijlstra A. Tetraspanins in cancer. In: Zent R, Pozzi A, editors. *Cell-extracellular matrix interactions in cancer*. New York: Springer; 2010. p. 217–43.
- Wang HX, Li Q, Sharma C, Knoblich K, Hemler ME. Tetraspanin protein contributions to cancer. *Biochem Soc Trans* 2011;39:547–52.
- Hong I-K, Jin Y-J, Byun H-J, Jeoung D-I, Kim Y-M, Lee H. Homophilic interactions of Tetraspanin CD151 up-regulate motility and matrix metalloproteinase-9 expression of human melanoma cells through adhesion-dependent c-Jun activation signaling pathways. *J Biol Chem* 2006;281:24279–92.
- Takeda Y, Li Q, Kazarov AR, Eparaud M, Elpek K, Turley SJ, et al. Diminished metastasis in tetraspanin CD151-knockout mice. *Blood* 2011;118:464–72.
- Zijlstra A, Lewis J, Degryse B, Stuhlmann H, Quigley JP. The inhibition of tumor cell intravasation and subsequent metastasis via regulation of in vivo tumor cell motility by the tetraspanin CD151. *Cancer Cell* 2008;13:221–34.
- Stipp CS, Kolesnikova TV, Hemler ME. EWI-2 is a major CD9 and CD81 partner and member of a novel Ig protein subfamily. *J Biol Chem* 2001;276:40545–54.
- Yáñez-Mó M, Barreiro O, Gonzalo P, Batista A, Megias D, Genis L, et al. MT1-MMP collagenolytic activity is regulated through association with tetraspanin CD151 in primary endothelial cells. *Blood* 2008;112:3217–26.
- Palmer DT, Zijlstra A. CD151. *UCSD-Nature Molecule Pages* 2011 (doi:10.1038/mp.a004123.01).
- Winterwood NE, Varzavand A, Meland MN, Ashman LK, Stipp CS. A critical role for tetraspanin CD151 in alpha3beta1 and alpha6beta4 integrin-dependent tumor cell functions on laminin-5. *Mol Biol Cell* 2006;17:2707–21.
- Kazarov AR, Yang X, Stipp CS, Sehgal B, Hemler ME. An extracellular site on tetraspanin CD151 determines alpha 3 and alpha 6 integrin-dependent cellular morphology. *J Cell Biol* 2002;158:1299–309.
- Novitskaya V, Romanska H, Dawoud M, Jones JL, Berditchevski F. Tetraspanin CD151 regulates growth of mammary epithelial cells in three-dimensional extracellular matrix: implication for mammary ductal carcinoma in situ. *Cancer Res* 2010;70:4698–708.
- Yang XH, Flores LM, Li Q, Zhou P, Xu F, Krop IE, et al. Disruption of laminin-integrin-CD151-focal adhesion kinase axis sensitizes breast cancer cells to ErbB2 antagonists. *Cancer Res* 2010;70:2256–63.
- Deng X, Li Q, Hoff J, Novak M, Yang H, Jin H, et al. Integrin-associated CD151 drives ErbB2-evoked mammary tumor onset and metastasis. *Neoplasia* 2012;14:678–89.
- Lau L-M, Wee JL, Wright MD, Moseley GW, Hogarth PM, Ashman LK, et al. The tetraspanin superfamily member CD151 regulates outside-in integrin alphaIIb beta3 signaling and platelet function. *Blood* 2004;104:2368–75.
- Sachs N, Kreft M, van den Bergh Weerman MA, Beynon AJ, Peters TA, Weening JJ, et al. Kidney failure in mice lacking the tetraspanin CD151. *J Cell Biol* 2006;175:33–9.
- Berditchevski F, Gilbert E, Griffiths MR, Fitter S, Ashman L, Jenner SJ. Analysis of the CD151-alpha3beta1 integrin and CD151-tetraspanin interactions by mutagenesis. *J Biol Chem* 2001;276:41165–74.
- Zhang XA, Kazarov AR, Yang X, Bontrager AL, Stipp CS, Hemler ME. Function of the tetraspanin CD151-alpha6beta1 integrin complex during cellular morphogenesis. *Mol Biol Cell* 2002;13:1–11.
- Yamada M, Tamura Y, Sanzen N, Sato-Nishiuchi R, Hasegawa H, Ashman LK, et al. Probing the interaction of tetraspanin CD151 with integrin alpha 3 beta 1 using a panel of monoclonal antibodies with distinct reactivities toward the CD151-integrin alpha 3 beta 1 complex. *Biochem J* 2008;415:417–27.
- Haeuw JF, Goetsch L, Bailly C, Corvaia N. Tetraspanin CD151 as a target for antibody-based cancer immunotherapy. *Biochem Soc Trans* 2011;39:553–8.
- Serru V, Le Naour F, Billard M, Azorsa DO, Lanza F, Boucheix C, et al. Selective tetraspanin-integrin complexes (CD81/alpha4beta1, CD151/alpha3beta1, CD151/alpha6beta1) under conditions disrupting tetraspanin interactions. *Biochem J [Internet]* 1999;340 (Pt 1):103–11.
- Geary SM, Cambareri AC, Sincoc PM, Fitter S, Ashman LK. Differential tissue expression of epitopes of the tetraspanin CD151 recognized by monoclonal antibodies. *Tissue Antigens* 2001;58:141–53.
- Sterk LMT, Geuijen CAW, van den Berg JG, Claessen N, Weening JJ, Sonnenberg A. Association of the tetraspanin CD151 with the laminin-binding integrins alpha3beta1, alpha6beta1, alpha6beta4 and alpha7-beta1 in cells in culture and in vivo. *J Cell Sci* 2002;115:1161–73.
- Chometon G, Zhang Z-G, Rubinstein E, Boucheix C, Mauch C, Aumailley M. Dissociation of the complex between CD151 and laminin-binding integrins permits migration of epithelial cells. *Exp Cell Res* 2006;312:983–95.
- Palmer TD, Lewis J, Zijlstra A. Quantitative analysis of cancer metastasis using an avian embryo model. *J Vis Exp* 51, e2815 (2011).
- Ossowski L, Reich E. Changes in malignant phenotype of a human carcinoma conditioned by growth environment. *Cell* 1983;33:323–33.
- Testa JE, Brooks PC, Lin JM, Quigley JP. Eukaryotic expression cloning with an antimetastatic monoclonal antibody identifies a tetraspanin (PETA-3/CD151) as an effector of human tumor cell migration and metastasis. *Cancer Res* 1999;59:3812–20.
- Ashby WJ, Wikswo JP, Zijlstra A. Magnetically attachable stencils and the non-destructive analysis of the contribution made by the underlying matrix to cell migration. *Biomaterials* 2012;33:8189–203.
- Marjoram RJ, Voss B, Pan Y, Dickeson SK, Zutter MM, Hamm HE, et al. Suboptimal activation of protease-activated receptors enhances alpha2beta1 integrin-mediated platelet adhesion to collagen. *J Biol Chem* 2009;284:34640–7.
- Cerami E, Gao J, Dogrusoz U, Gross BE, Sumer SO, Aksoy BA, et al. The cBio cancer genomics portal: an open platform for exploring multidimensional cancer genomics data. *Cancer Discov* 2012;2:401–4.
- Chandran UR, Ma C, Dhir R, Bisceglia M, Lyons-Weiler M, Liang W, et al. Gene expression profiles of prostate cancer reveal involvement of multiple molecular pathways in the metastatic process. *BMS*;7:21.
- Varambally S, Yu J, Laxman B, Rhodes DR, Mehra R, Tomlins SA, et al. Integrative genomic and proteomic analysis of prostate cancer reveals signatures of metastatic progression. *Cancer Cell* 2005;8:393–406.
- Tomlins SA, Mehra R, Rhodes DR, Cao X, Wang L, Dhanasekaran SM, et al. Integrative molecular concept modeling of prostate cancer progression. *Nat Genet* 2007;39:41–51.

34. Taylor BS, Schultz N, Hieronymus H, Gopalan A, Xiao Y, Carver BS, et al. Integrative genomic profiling of human prostate cancer. *Cancer Cell* 2010;18:11–22.
35. Dezso Z, Nikolsky Y, Sviridov E, Shi W, Serebriyskaya T, Dosymbekov D, et al. A comprehensive functional analysis of tissue specificity of human gene expression. *BMC Biol* 2008;6:49.
36. Fogerty FJ, Akiyama SK, Yamada KM, Mosher DF. Inhibition of binding of fibronectin to matrix assembly sites by anti-integrin (alpha 5 beta 1) antibodies. *J Cell Biol* 1990;111:699–708.
37. Offermanns S. Activation of platelet function through G protein-coupled receptors. *Circ Res* 2006;99:1293–304.
38. Nishiuchi R, Murayama O, Fujiwara H, Gu J, Kawakami T, Aimoto S, et al. Characterization of the ligand-binding specificities of integrin alpha3beta1 and alpha6beta1 using a panel of purified laminin isoforms containing distinct alpha chains. *J Biochem* 2003;134:497–504.
39. Copeland BT, Bowman MJ, Ashman LK. Genetic ablation of the tetraspanin Cd151 reduces spontaneous metastatic spread of prostate cancer in the TRAMP model. *Mol Cancer Res* 2012;11:95–105.
40. Uhlen M, Oksvold P, Fagerberg L, Lundberg E, Jonasson K, Forsberg M, et al. Towards a knowledge-based Human Protein Atlas. *Nat Biotechnol*. 2010;28:1248–50.
41. Yang XH, Richardson AL, Torres-Arzayus MI, Zhou P, Sharma C, Kazarov AR, et al. CD151 accelerates breast cancer by regulating alpha 6 integrin function, signaling, and molecular organization. *Cancer Res* 2008;68:3204–13.
42. Liu L, He B, Liu WM, Zhou D, Cox JV, Zhang XA. Tetraspanin CD151 promotes cell migration by regulating integrin trafficking. *J Biol Chem* 2007;282:31631–42.
43. Ke H, Wang P, Yu W, Liu X, Liu C, Yang F, et al. Derivation, characterization and gene modification of cynomolgus monkey mesenchymal stem cells. *Differentiation* 2009;77:256–62.
44. Simpson KJ, Selfors LM, Bui J, Reynolds A, Leake D, Khvorova A, et al. Identification of genes that regulate epithelial cell migration using an siRNA screening approach. *Nat Cell Biol* 2008;10:1027–38.
45. Lammerding J, Kazarov AR, Huang H, Lee RT, Hemler ME. Tetraspanin CD151 regulates alpha6beta1 integrin adhesion strengthening. *Proc Natl Acad Sci USA* 2003;100:7616–21.
46. Tsujino K, Takeda Y, Arai T, Shintani Y, Inagaki R, Saiga H, et al. Tetraspanin CD151 protects against pulmonary fibrosis by maintaining epithelial integrity. *Am J Respir Crit Care Med* 2012;186:170–80.
47. Palecek SP, Loftus JC, Ginsberg MH, Lauffenburger DA, Horwitz AF. Integrin-ligand binding properties govern cell migration speed through cell-substratum adhesiveness. *Nature* 1997;385:537–40.
48. Sachs N, Sonnenberg A. Cell–matrix adhesion of podocytes in physiology and disease. *Nat Rev Nephrol* 2013;9:200–10.
49. Dedhar S, Saulnier R, Nagle R, Overall CM. Specific alterations in the expression of alpha 3 beta 1 and alpha 6 beta 4 integrins in highly invasive and metastatic variants of human prostate carcinoma cells selected by in vitro invasion through reconstituted basement membrane. *Clin Exp Metastasis* 1993;11:391–400.
50. Varzavand A, Drake JM, Svensson RU, Herndon ME, Zhou B, Henry MD, et al. Integrin  $\alpha 3 \beta 1$  regulates tumor cell responses to stromal cells and can function to suppress prostate cancer metastatic colonization. *Clin Exp Metastasis* 2013;30:541–52.

# Cancer Research

The Journal of Cancer Research (1916–1930) | The American Journal of Cancer (1931–1940)

## Integrin-Free Tetraspanin CD151 Can Inhibit Tumor Cell Motility upon Clustering and Is a Clinical Indicator of Prostate Cancer Progression

Trenis D. Palmer, Carlos H. Martínez, Catalina Vasquez, et al.

*Cancer Res* 2014;74:173-187. Published OnlineFirst November 12, 2013.

**Updated version** Access the most recent version of this article at:  
doi:[10.1158/0008-5472.CAN-13-0275](https://doi.org/10.1158/0008-5472.CAN-13-0275)

**Supplementary Material** Access the most recent supplemental material at:  
<http://cancerres.aacrjournals.org/content/suppl/2013/11/12/0008-5472.CAN-13-0275.DC1.html>

**Cited Articles** This article cites by 47 articles, 22 of which you can access for free at:  
<http://cancerres.aacrjournals.org/content/74/1/173.full.html#ref-list-1>

**Citing articles** This article has been cited by 1 HighWire-hosted articles. Access the articles at:  
<http://cancerres.aacrjournals.org/content/74/1/173.full.html#related-urls>

**E-mail alerts** [Sign up to receive free email-alerts](#) related to this article or journal.

**Reprints and Subscriptions** To order reprints of this article or to subscribe to the journal, contact the AACR Publications Department at [pubs@aacr.org](mailto:pubs@aacr.org).

**Permissions** To request permission to re-use all or part of this article, contact the AACR Publications Department at [permissions@aacr.org](mailto:permissions@aacr.org).